Journal of Polymers and the Environment
https://doi.org/10.1007/s10924-024-03287-5

ORIGINAL PAPER

Green and Atom Economical Route to High Compressive Strength Lignin Oil-Sulfur Composites

Katelyn A. Tisdale[1] · Nawoda L. Kapuge Dona[1] · Charini P. Maladeniya[1,2] · Rhett C. Smith[1]

Accepted: 3 April 2024

Abstract

Lignin is the most abundant natural source of aromatics but remains underutilized. Elemental sulfur is a plentiful by-product of fossil fuel refining. Herein we report a strategy for preparing a durable composite by the one-pot reaction of elemental sulfur and lignin oil comprising lower molecular weight lignin derivatives. A lignin oil-sulfur composite ($\mathbf{LOS_{90}}$) was prepared by reacting 10 wt. % lignin oil with 90 wt. % elemental sulfur. The composite could be remelted and reshaped over several cycles without loss of properties. Results from the study showed that $\mathbf{LOS_{90}}$ has properties competitive with or exceeding values for commercial ordinary Portland cement and brick formulations. For example, $\mathbf{LOS_{90}}$ displayed impressive compressive strength (22.1 MPa) and flexural strength (5.7 MPa). $\mathbf{LOS_{90}}$ is prepared entirely from waste materials with 98.5% atom economy of composite synthesis, a low *E* factor of 0.057, and lignin char as the only waste product of the process for its preparation. These results suggest the potential applications of lignin and waste sulfur in the continuous efforts to develop more recyclable and sustainable materials.

Keywords Bio oil · Biomass · Sulfur utilization · Composites · Lignin

Introduction

Lignin is a highly underutilized commodity available from lignocellulosic agricultural biomass waste. Over 5 billion metric tons of lignin waste are produced from pre-consumer biomass annually [1]. Paper production also contributes approximately 600,000 tons per year of additional lignin waste [2]. In terms of potential commodities for carbon sequestration, lignin notably sequesters ~ 30% of organic carbon on the planet [1]. A barrier to lignin utilization is its complex structure deriving from its biosynthesis that links primarily 4-*p*-coumaryl alcohol, coniferyl alcohol, and sinapyl alcohol, giving rise to the *p*-hydroxyphenyl, guaiacyl, and syringyl subunits, respectively, in lignins (Fig. 1) [3]. Not only is lignin a mixture of these diverse subunits, but their relative contribution to a particular lignin also varies with the part of the plant from which it is derived and the plant species. Lignin from grasses, for example, contains significant quantities of all three structural subunits, while hardwood lignin features significant quantities of guaiacyl and syringyl subunits but few *p*-hydroxyphenyl subunits, and softwood lignins feature primarily guaiacyl subunits [1].

Efficient valorization of lignin involves both "upstream" and "downstream" processes. Upstream processes includes the separation and isolation of lignin, lignin bioengineering, and the catalytic conversion of lignin, while downstream processes includes both lignin depolymerization as well as lignin upgrading [4]. Among the most promising efforts to improve lignin utilization is through depolymerization, giving bio-oils or lignin oils [5]. In regards to sample preparation, it is important to find green methods when considering solvent consumption. A few of these "green" solvents used for extraction procedures include, supercritical fluids, bio-based solvents, and liquified gases. Supercritical fluid extraction (SFE) involves shorter extraction time, improved efficiency, better selectivity, and the extracting solvent is easy to remove. Liquified gases such as butane and n-propane are advantageous because they require gentle pressure (< 1 MPa) to stay a liquid and is easily evaporated at low temperatures. Thus, liquified gas extraction can be performed at room temperature with little energy consumption

✉ Rhett C. Smith
rhett@clemson.edu

[1] Department of Chemistry, Clemson University, Clemson, SC 29634, USA

[2] Oak Ridge National Labs, Oak Ridge, TN 37830, USA

Published online: 29 April 2024

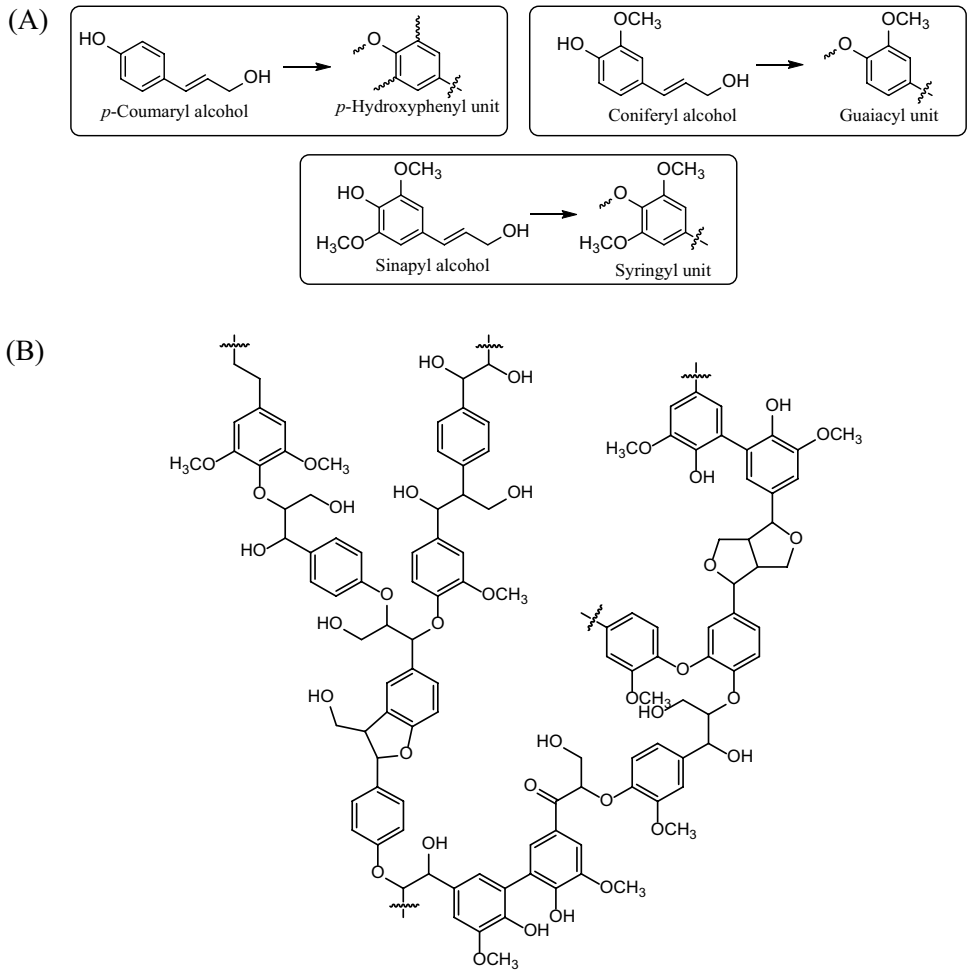

Fig. 1 Lignin biosynthetic precursors (**A**) and structure showing features of some lignins (**B**)

and the extracts containing a negligible residual amount of solvent. Bio-based solvents can be obtained from a wide variety of biomass sources. They can be obtained through methods such as extracting vegetable oils, carbohydrate fermentation, and the steam distillation of wood [6]. Ethanol is a solvent of particular interest due to its availability via the fermentation of renewable resources such as starches, sugars, and lignocellulosics. Ethanol is also fairly low cost and readily available [7].

A recent report [8] on mild thermolytic solvolysis of lignin to yield a solubilized lignin oil was particularly attractive for the current work because the process could be accomplished at low temperatures (100–350 °C), using preferred green solvents [9] like ethanol. With ethanol at only 100 °C, this process conveniently accomplished conversion of 64 wt. % of lignin to lignin oil.

Elemental sulfur is another abundant and underemployed by-product of human industry, and is produced at a rate of 70 million metric tons per year from fossil fuel refining [10, 11]. In recent years, we have reported several efforts to prepare composites combining lignin and sulfur via the inverse vulcanization method [12–14]. It has proven difficult to obtain inverse vulcanized polymers that possess concurrent high strength, toughness, and elongation [15]. Additional mechanisms for S–C bond-formation will not only expand the organic substrate scope for preparing high sulfur-content materials (HSMs) but may also achieve more favorable mechanical properties.

Because classic inverse vulcanization requires olefins, prior lignin-sulfur composite synthesis required modification of lignin with olefins before reaction with sulfur [13, 14]. Allyl-derivatized lignin composites $\mathbf{LS_x}$ (x = wt. % sulfur in monomer feed, varied from 80 to 99) and $\mathbf{ELS_x@T}$ (where x = wt. % sulfur in the monomer feed, varied from 80 to 90, and T is the reaction temperature in °C) achieved the goal of producing high strength lignin-sulfur composites, but additional synthetic / separations / use of non-green solvents detract from the greenness, atom economy, and affordability of those processes.

A more efficient one-pot synthesis of lignin-sulfur composite $\mathbf{CLS_{90}}$ was developed by reacting sulfur (90 wt. %) with chlorolignin (10 wt. %), a waste product of paper/pulping. Preparation of $\mathbf{CLS_{90}}$ occurred via radical-induced aryl halide-sulfur polymerization (RASP, Scheme 1B) rather

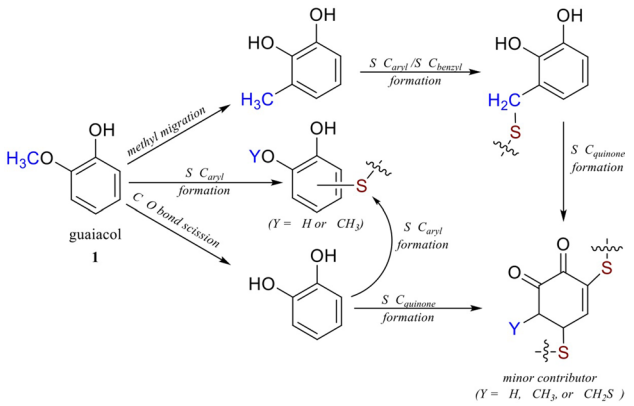

Scheme 1 Major S–C bond-forming reactions in the formation of $\mathbf{GS_{80}}$ from sulfur and guaiacol

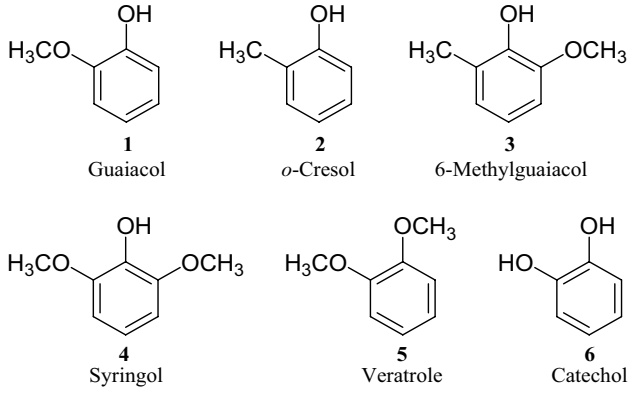

Fig. 2 Lignin derivatives/model compounds reacted with elemental sulfur in the current study to inform on the range of chemistries operational during synthesis of $\mathbf{LOS_{90}}$ from lignin oil

than inverse vulcanization [16]. RASP involves S–C_{aryl} bond formation via thermal generation of aryl radicals via C–Halide σ-bond scission and subsequent reaction of aryl halides with S–S bonds. Although this process proved valuable as a simple one-pot synthesis of durable composites from two industrial waste products, it produces 0.5 equivalents of toxic S_2Cl_2 for each S–C bond formed, making RASP generally less ecologically desirable and less atom economical than inverse vulcanization.

Given results from the aforementioned lignin-sulfur composites ($\mathbf{LS_x}$, $\mathbf{ELS_x}$**@T**, and $\mathbf{CLS_{90}}$), it was of interest to investigate other possible S–C bond-forming reactions involving lignin derivatives. Lignin itself does not contain alkenes or halogens, but features a high abundance of anisole derivative subunits. We recently unveiled new S–C bond-forming mechanisms that occur when elemental sulfur is heated above 220 °C with anisole derivatives like *O*,*O*′-dimethylbisphenol A, [17] guaiacol, [14] and others [18]. These studies revealed a range S–C bond-forming processes. The S–C bond-forming reaction of guaiacol (80 wt. %) and sulfur (20 wt. %) at 230 °C, for example, gave composite $\mathbf{GS_{80}}$, comprising sulfur catenate crosslinkers attached to aryl units (Scheme 1) [14]. This is especially pertinent to the current study because guaiacol is a common constituent of many lignin oils. $\mathbf{GS_{80}}$ exhibited improved tensile strength and elongation at break compared to most HSMs derived from renewable organics that had been reported at the time of its synthesis.

Given the range of S–C bond-forming reactions unveiled in previous studies and the ability of such bond-forming reactions to stabilize composites of guaiacol and sulfur, we hypothesized that a durable composite would be attainable by the reaction of elemental sulfur with lignin oil as an alternative to whole lignin that can be used without prior derivatization. Herein, composite $\mathbf{LOS_{90}}$ was synthesized by heating lignin oil (10 wt. %) with elemental sulfur (90 wt. %) at 230 °C for 24 h. A series of model compounds (Fig. 2) featuring functional groups present in lignin subunits or thermal degradation products previously observed (Scheme 2) were reacted with elemental sulfur under identical conditions to further inform on S–C bond-forming reactions operable in $\mathbf{LOS_{90}}$. Properties of composite $\mathbf{LOS_{90}}$ were characterized using differential scanning calorimetry (DSC, mechanical test stand analysis, thermogravimetric analysis (TGA), infrared spectroscopy, flexural strength analysis, and scanning electron microscopy with elemental mapping by energy-dispersive X-ray analysis (SEM–EDX). These studies reveal that $\mathbf{LOS_{90}}$ is a microscopically homogeneous composite with good thermal stability and compressive strength higher than is required of ordinary Portland cement for residential building foundations.

Materials and Methods

Materials

Sulfur powder (99.5%) was purchased from Alfa Aesar. Compounds 6-methylguaiacol (> 98%) and 1,2-dimethoxybenzene (99%) were purchased from TCI (Tokyo Chemical Industry). Compounds *o*-cresol (> 99%) and syringol (99%) were purchased from Sigma Aldrich. Catechol (99%) was purchased from Acros Organics. These chemicals were used without further purification. The lignin oil used in this study was produced by a reported method using thermal solvolysis of kraft lignin in ethanol [8].

General Considerations and Instrumentation

All ^{1}H NMR spectra were recorded on a Bruker Avance spectrometer operating at 300 MHz.

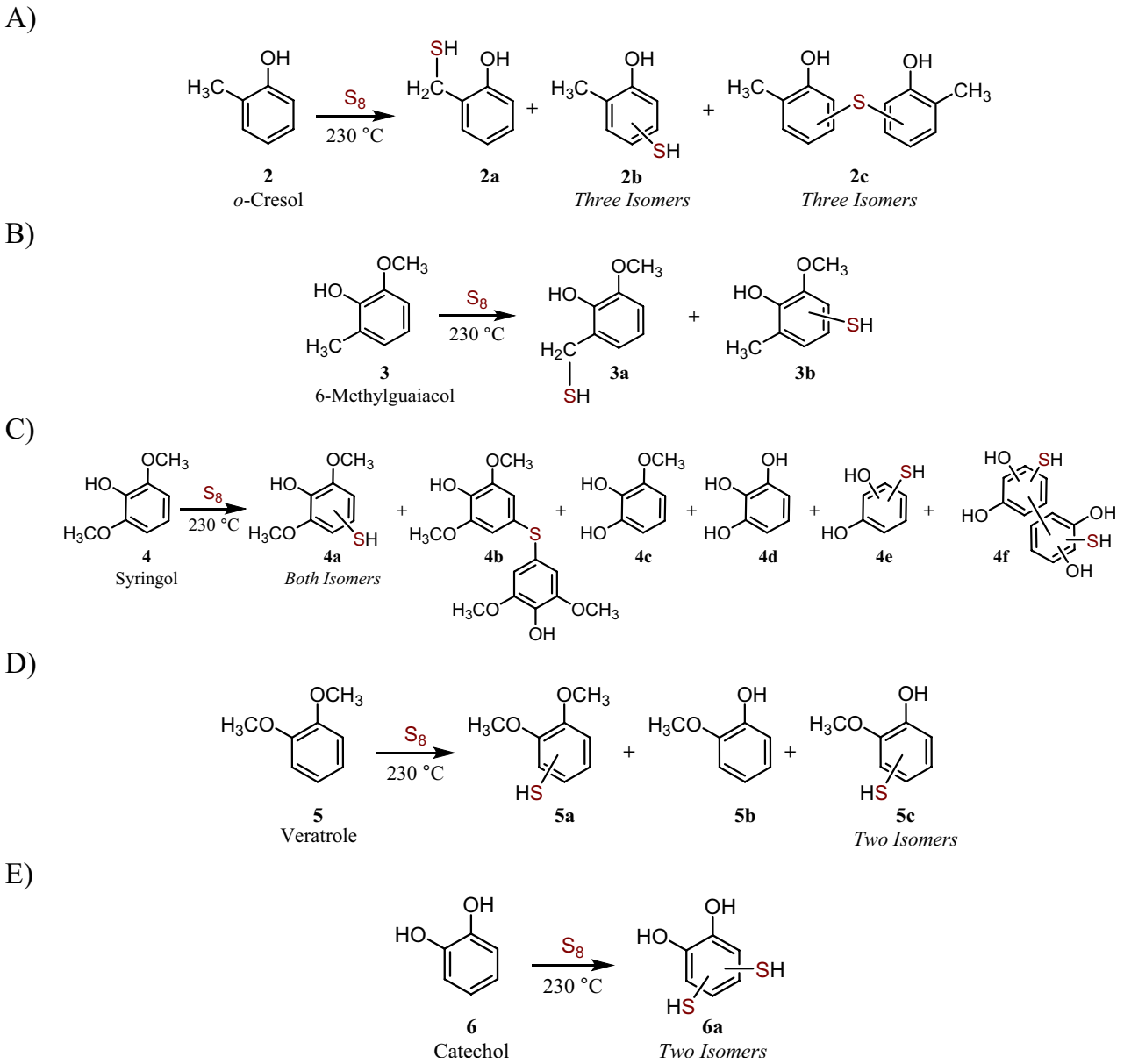

Scheme 2 Reaction of model compounds **2–6** with elemental sulfur provides insight into reactivity between elemental sulfur and variably-functionalized aryl units

GC–MS studies were carried out on a Shimadzu QP2010SE system with an auto-injector (AOC-20i) equipped with the mass selective detector, having an interface temperature of 250 °C, a solvent cut time of 3.00 min, threshold of 70 eV and mass range of 45 to 900 m/z. Compounds were separated using a SH-Rxi-5 MS capillary column (Restek Company, Bellefonte, USA: crossbond 5% diphenyl/ 95% dimethyl polysiloxane) having dimensions 30 m (length) × 0.25 mm (diameter) × 0.25 µm (film thickness). The temperature of the injector was initialized to 250 °C. The temperature was programmed to 50 °C for 1 min, then from 50 °C to 320 °C at a rate of 20 °C/min, then held at 320 °C for 4 min.

Fourier transform infrared spectra were obtained using an IR instrument (Shimadzu IRAffinity-1S) with an ATR attachment. Scans were collected over the range 400–4000 cm^{-1} at ambient temperature with a resolution of 8 cm^{-1}.

SEM was acquired on a Schottky Field Emission Scanning Electron Microscope SU5000 operating in variable pressure mode with an accelerating voltage of 15 keV.

Compressional strength measurements were undertaken with cylinders using a Mark-10 ES30 (USA) Manual Test Stand equipped with a Mark 10 M3-200 Force Gauge (USA) by a modified ASTM C39 standard. The **LOS_{90}** composites were melted, formed in molds, and then cooled to room temperature. The cylinders were aged for 4 d before they underwent compressional strength testing. The stability for these materials longer-term is unknown.

Flexural strength analyses were carried out using a Mettler Toledo DMA 1 STARe System in single cantilever mode. The samples were made using silicon resin moulds. The samples dimensions were 1.5 × 10.7 × 5.0 mm. The temperature was 25 °C and the clamping force was 1 cN m. The samples were tested in triplicates and the reported flexural strength and moduli is an average of the three trials.

TGA data were recorded (Mettler Toledo TGA 2 STARe System) over the range 20–800 °C with a heating rate of 10 °C·min^{-1} under a flow of N_2 (100 mL·min^{-1}).

DSC data were recorded using a Mettler Toledo DSC 3 STARe System with a temperature range of –60 °C to 140 °C with a heating rate of 10 °C·min^{-1} under a flow of N_2 (200 mL·min^{-1}). Each DSC measurement was performed over three heating and cooling cycles. The data reported herein are from the third cycle. The first cycle removes any solvent impurities. The melting and crystallization transitions and the glass-transition temperature were seen in during the third cycle. The change of percentage crystallinity between the sulfur and the composites was calculated from the DSC data utilizing the following equation:

$$\Delta\chi_c = 1 - \left\{ \frac{\Delta H_m - \Delta H_{cc}}{\Delta H_{m(S)} - \Delta H_{cc(S)}} \right\} \times 100\%$$

where ΔX_c is change of percentage crystallinity with respect to sulfur, ΔH_m is the melting enthalpy of the composite, ΔH_{cc} is the cold crystallization enthalpy of the composite, $\Delta H_{m(S)}$ is the melting enthalpy of sulfur, and $\Delta H_{cc(S)}$ is the cold crystallization enthalpy of sulfur.

Synthetic Procedure Safety Note

CAUTION: Heating elemental sulfur with organics can result in the formation of H_2S or other gases. Such gases can be toxic, foul-smelling, and corrosive. Temperature must be carefully controlled to prevent thermal spikes, contributing to the potential for H_2S or other gas evolution. Rapid stirring shortened heating times, and very slow addition of reagents can help avoid unforeseen temperature spikes.

Model Compound Reactivity Studies

For each of the compounds shown in Fig. 2, 1.600 g elemental sulfur and 0.400 g of the organic compound were added directly into a glass pressure tube under an atmosphere of dry nitrogen gas in a VTI glovebox. Each pressure tube was equipped with a magnetic stir bar and sealed under N_2 with a Teflon screwcap having a Viton O-ring. Each tube was placed into an oil bath heated to 230 °C. Heating was continued for 24 h with continuous stirring by a magnetic stir bar. After 24 h of heating the pressure tubes were cooled to room temperature before opening. No mass loss was observed from any of the tubes. For ^{1}H NMR analysis, 50 mg of each product mixture was placed in 1.0 mL of $CDCl_3$ and shaken to facilitate dissolution. The mixture was then filtered through a 0.2 µm PTFE syringe filter and transferred to the NMR tube. GC–MS samples, 20 mg of each reaction mixture was extracted into CH_2Cl_2 followed by filtration through a 0.2 µm PTFE syringe filter.

Synthesis of LOS_{90}

Elemental sulfur (45.0 g) was added to a large Erlenmeyer flask and then placed in an oil bath. The sulfur was then heated to 180 °C and allowed to melt until a reddish liquid was formed. The lignin oil (5.00 g) was then added to the flask and covered with aluminum foil. Rapid mechanical stirring was then applied. The temperature was then increased to 230 °C. The mixture was heated for 2 h under continuous rapid mechanical stirring. Within the 2 h, the reaction mixture turned dark brown in color and appeared homogeneous. After the 2 h, the stirring was stopped, and the reaction was removed from the heat. The resulting product was allowed to cool to room temperature, forming a dark brown solid. To form the cylinders for compressive strength tests and rectangular prisms for flexural strength tests, the product was remelted at 180 °C then poured into molds and cooled to room temperature. Elemental analysis theoretical: found: C 3.08, H 0.16, S 94.17.

Dark Sulfur Quantification

This procedure follows a modified literature procedure from Hasell's group [19] employing toluene to extract and quantify dark sulfur. Extraction of dark- sulfur was performed by suspending 100 mg of finely ground **LOS_{90}** in 20 mL of toluene in a centrifuge tube. After an hour, the tube centrifuged for approximately 30 s, allowing the solid to collect at the bottom of the tube. The supernatant was then transferred by pipette into a round bottom flask. The toluene was evaporated from each fraction under reduced pressure and both solids weighed to determine the amount of dark sulfur and insoluble material. Elemental analysis confirmed that the soluble material was > 98.5% sulfur.

Results and Discussion

Synthesis and Chemical Characterization of Composite

The lignin oil used in this study was produced by a reported method using thermal solvolysis of kraft lignin in ethanol (1:5 w/v ratio) at 100 °C. This route to lignin oil was selected because of the relatively low temperature and use of a preferred green solvent [8]. Analyses of the lignin oil by 2D HSQC NMR spectrometry (Fig. S1, Supplementary Material) and MALDI (Fig. S2, Supplementary Material) support the same composition as was previously reported for lignin oils prepared by this method (illustrative structural subunits are provided in Fig. S3 in the Supplementary Material). The fragmentation of the whole lignin into lower molecular weight monomers was further confirmed by MALDI-TOF spectrometry, which verified the presence of significant quantities of whole lignin as well as of higher oligomers consistent with reported composition of the lignin oils prepared by this method. (Fig. S2 in the Supplementary Material).

Preparation of **LOS$_{90}$** involved the reaction of lignin oil (5.0 g, 10 wt. %) and sulfur (45 g, 90 wt. %). Sulfur was first melted in an Erlenmeyer flask and heated to 180 °C, followed by the addition of lignin oil with rapid mechanical stirring. The temperature was increased to 230 °C under continuous stirring and the mixture was stirred for 2 h while the top of the flask was covered with aluminum foil. The mixture was visually homogenous throughout the heating period, allowing a much shorter reaction time than the 24 h of heating required for synthesis of lignin-sulfur composite **LS$_x$**. **LOS$_{90}$** solidified into a dark brown, remeltable solid after cooling to room temperature, in an isolated yield of 98.5% of **LOS$_{90}$**. Heating sulfur with organics that have readily abstractable H atoms can produce toxic hydrogen sulfide gas, with attendant mass loss of up to 34% [20]. The high isolated yield of **LOS$_{90}$** and the lack of discoloration of the aluminum foil covering both indicate negligible if any hydrogen sulfide generation in the current case. Upon melting, the material was poured into molds and allowed to cool to room temperature to form samples for both compressive and flexural strength tests.

In HSMs the sulfur present as crosslinking –S$_x$– chains is generally accompanied by small quantities of physically entrapped sulfur species not covalently linked to the organic comonomers. The physically entrapped sulfur is known as dark sulfur and its contribution to an HSM is generally determined by its extraction and quantification either by UV–vis spectroscopy or by evaporating the extraction solvent and quantifying the mass directly [19, 21]. In the current case, dark sulfur was extracted with toluene, followed by evaporation of the toluene and weighing the extractable material. Elemental analysis was also performed on the soluble fraction, confirming it was > 98% sulfur. The composite **LOS$_{90}$** comprised 76 wt. % insoluble material and 23 wt. % dark sulfur, demonstrating high incorporation of sulfur into the polymer network. **LOS$_{90}$** exhibits a similar dark sulfur content to the 16 wt. % dark sulfur content of **LS$_{90}$** (a composite prepared from allylated lignin with 90 wt. % sulfur).

Evidence of C–S bond formation between the lignin oil constituents and the polymeric sulfur was observed by infrared spectroscopy (Fig. 3). A peak was observed at 660 cm^{-1} indicating the C–S stretch [22–24]. The IR spectra (Fig. S4, Supplementary Material) also confirmed that **LOS$_{90}$** retained characteristic peaks for the lignin oil such as O–H stretching (3200–3500 cm^{-1}), C–H stretching (2930 cm^{-1}), and C–O stretches (1030–1200 cm^{-1}).

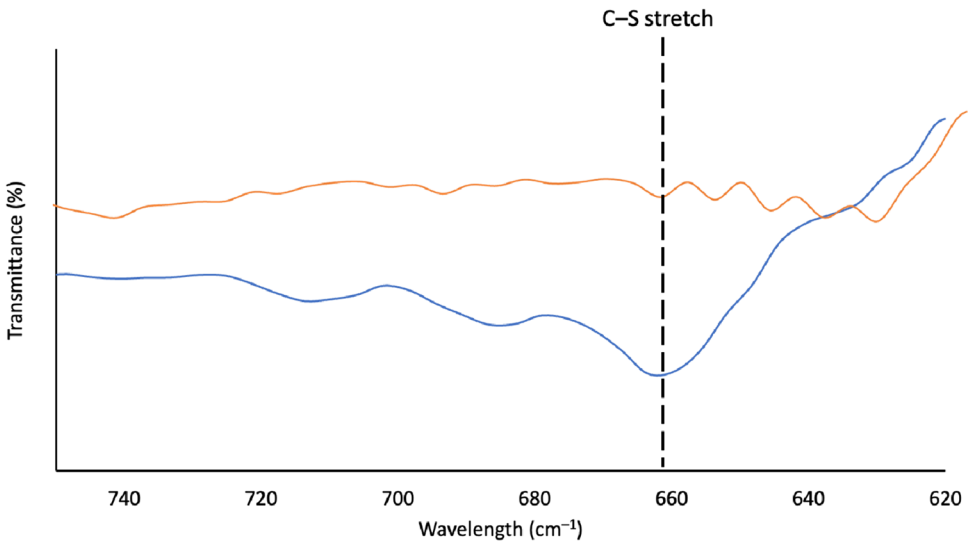

Fig. 3 Portion of the FT-IR spectrum of **LOS$_{90}$** (blue trace) compared to that of lignin oil (orange trace). Full spectra are provided in the Supplementary Material (Fig. S4) (Color figure online)

Scanning electron microscopy (SEM, Fig. S5, Supplementary Material) imaging with elemental mapping by energy dispersive X-ray analysis (EDX) was performed to assess the distribution of components in the **LOS$_{90}$** composite (Fig. 4). SEM/EDX data showed homogeneous distribution of S, C, and O. Small dots of silica-rich material observed are residue from the SEM sample preparation.

Model Compound Reactivity Studies

Compounds **2**–**6** (Fig. 1) were selected as models of lignin oil components that may engage in S–C bond-forming reactions like those we previously reported for guaiacol (1, Scheme 1C). Each compound **2**–**6** was reacted with elementals sulfur under conditions identical to those used to prepare **LOS$_{90}$**. Following reaction, the soluble compounds were extracted under conditions that will give thiols at each position where a crosslinking –S$_x$– chain is expected to attach to the organic scaffold in such units in **LOS$_{90}$**. This allowed for identification of small molecular species present in the reaction mixtures by GC–MS analysis (Figs. S6–S65 in the Supplementary Material). The observed chemistry is summarized in Scheme 2.

Compounds **2b**, **3b**, **4a**, and **5a** each result from forming one S–C$_{aryl}$ bond. There does not appear to be a strong regioselectivity trend for the formation of these S–C$_{aryl}$ bonds, as all three of the possible regioisomers of **2b**, one of the three possible regioisomers of **3b**, both regioisomers of **4a**, one regioisomer of **5a**, and two of the four regioisomers of **5c** were observed. Two other products featuring one new S–C$_{aryl}$ bond each, **4e** and **5c**, were also observed, but S–C bond formation was accompanied by additional backbone modifications described below.

Several species featuring two S–C$_{aryl}$ bonds were also observed, modelling modes of crosslinking in **LOS$_{90}$**. A sulfur atom joins two aryl rings in compounds **2c** (three

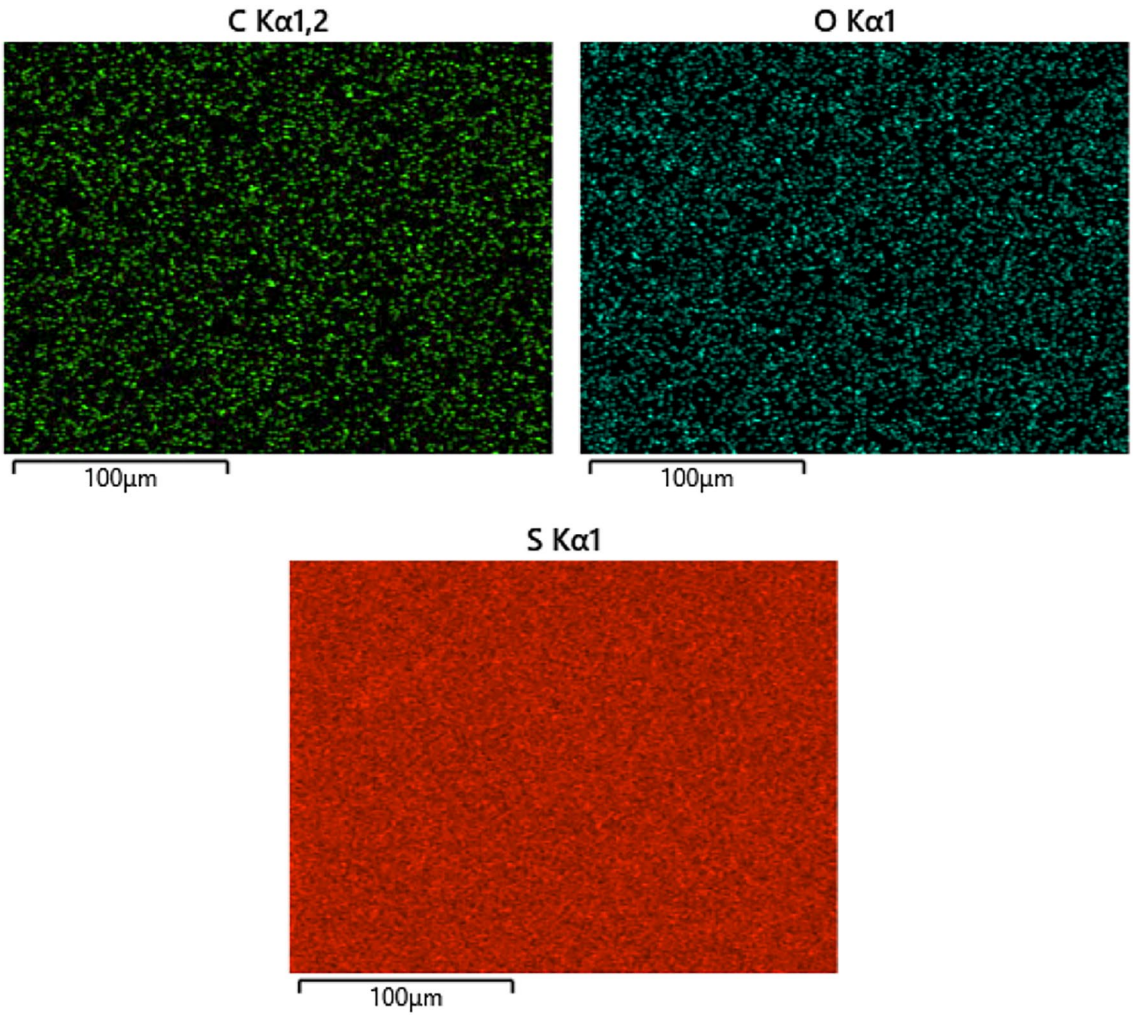

Fig. 4 Elemental mapping of carbon (green, upper left), oxygen (blue, upper right), and sulfur (lower right) in **LOS$_{90}$** by energy dispersive X-ray analysis (EDX) (Color figure online)

regioisomers observed) and **4b**. For **4b**, only one regioisomer forms as a result of the steric encumbrance at other potential attachment sites. Similar diaryl thioether derivatives **1b** were reported from reaction of **1** with sulfur (Scheme 1C).

In one instance the formation of two S–C_{aryl} bonds to the same aryl ring was observed to give product **6a** (two regioisomers observed). One compound, **4f**, was observed in which two aryl rings were joined by a new C_{aryl}–C_{aryl} bond, and each aryl ring featured a thiol substituent as a result of two newly-formed S–C_{aryl} bonds.

Some products observed from reactions of **4** and **5** involve scission of the methoxy C–O σ-bond, also observed in reactions of guaiacol with sulfur (Scheme 1C). Sulfur is not required to facilitate this pathway, however, as heating pure **4** without sulfur leads to similar C–O σ-bond scission [25]. Loss of one or both methyl groups from **4** led to products **4c** and **4d**, while loss of one of the methyl groups from **5** led to **5b**. In addition to the loss of methyl groups, **4** also underwent O–C_{aryl} σ-bond scission with a net loss of one hydroxy/methoxy unit from the structure, accompanied by S–C_{aryl} bond formation to give **4e**. Loss of methoxy groups via O–C_{aryl} σ-bond scission is also a known thermal decomposition route for **4** in the absence of sulfur [25].

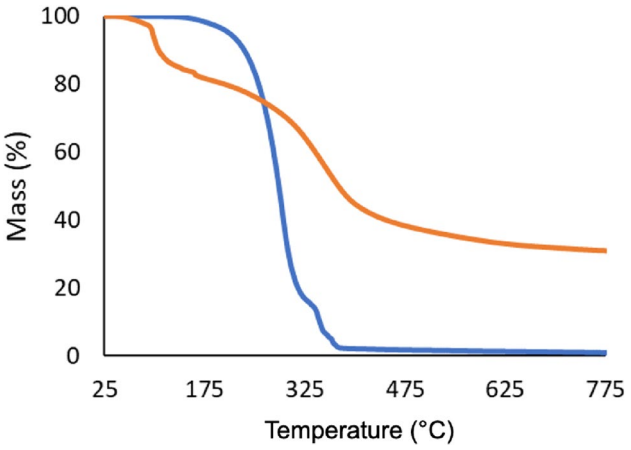

Fig. 5 Thermogravimetric analysis (TGA) traces for **LOS_{90}** (blue trace) and lignin oil (orange trace) (Color figure online)

Thermal and Morphological Properties of LOS_{90}

The thermal stability of lignin oil and **LOS_{90}** were assessed using thermogravimetric analysis (TGA, Fig. 5 and Table 1).

The lignin oil decomposed over a broad temperature range and showed three decomposition events at 93 °C, 159 °C, and 309 °C. The first decomposition temperature is attributable to loss of entrapped ethanol (observed by NMR analysis and not removable under vacuum) and water. The decomposition feature with onset at 159 °C is due to the

Table 1 Thermal and morphological properties of the lignin oil-sulfur composites **LOS_{90}** with comparison to sulfur and other composites

Materials	T_d[a]/°C	T_m[b]/°C	$T_{g,DSC}$[c]/°C	ΔH_m J/g	ΔH_{cc} J/g	Percent crystallinity[d]	References
LOS_{90}[e]	229	114	–36	26	ND	57	Current work
LS_{80}[f]	236	118	–34	30	25	8	[13]
LS_{85}[f]	235	118	–35	34	13	40	[13]
LS_{90}[f]	237	117	ND	34	ND	67	[13]
LS_{95}[f]	235	107	ND	37	ND	63	[13]
LS_{99}[f]	233	113	ND	47	ND	91	[13]
GS_{80}[g]	264	ND	–30	ND	ND	ND	[15]
ELS_{80}@180[h]	231	117	–37	ND	ND	ND	[14]
ELS_{90}@180[h]	230	117	–37	ND	ND	ND	[14]
ELS_{90}@230[h]	234	117	–37	ND	ND	ND	[14]
S_8[i]	228/229	119	ND	45	ND	100	[40]

[a]The temperature at which 5% mass [loss] is observed

[b]The peak temperature at the peak maximum of the endothermic melting

[c]Glass transition temperature

[d]The reduction of percent crystallinity of each sample calculated with respect to sulfur (normalized to 100%)

[e]Lignin Oil (10 wt. %) and elemental sulfur (90 wt. %)

[f]**LS_x** composites consisting of 10 wt. % allyl-derivatized lignin and elemental sulfur where x = wt. % sulfur in monomer feed, varied from 80 to 99

[g]Composites consisting of guaiacol (20 wt. %) and elemental sulfur (80 wt. %)

[h]**ELS_x@T** composites consisting of esterified lignin and elemental sulfur where x = wt. % sulfur in the reaction mixture, varied from 80 to 90, and T is the reaction temperature in °C

[i]Elemental sulfur

degradation of the propanoic side chains in whole lignin oligomers, while the decomposition feature with onset of at 309 °C is attributed to the cleavage of β–β and C–C linkages in lignin oil oligomers [26]. The TGA trace for **LOS$_{90}$** showed a single decomposition event revealing a decomposition temperature (T_d) of 229 °C, typical for HSMs and for elemental sulfur (T_d of 229 °C) and attributable to sublimation of entrapped *cyclo*-S_8 in **LOS$_{90}$**. The smaller decomposition event at > 300 °C in **LOS$_{90}$** is attributable to decomposition of the lignin oil-derived organics.

Differential scanning calorimetry (DSC, Fig. 6) of the **LOS$_{90}$** composites revealed thermal transitions associated with *cyclo*-S_8 and polymeric sulfur. **LOS$_{90}$** exhibited a melting peak expected for *cyclo*-S_8 at 114 °C, consistent with the effective removal of entrapped *cyclo*-S_8 by toluene extraction. The shoulder to the low-temperature side of the prominent melt transition is attributable to sulfur's α-to-β phase transition. A glass transition temperature (T_g) was also observed in the third heating cycle at –36 °C, diagnostic for polymeric sulfur. The melting and cold crystallization enthalpies was used to calculate the percent crystallinity of **LOS$_{90}$** compared to orthorhombic α-sulfur. Based on these data, the crystallinity of **LOS$_{90}$** was 57% that of α-sulfur, quite similar to that of **LS$_{90}$** (67%) that, like **LOS$_{90}$**, comprises 90 wt. % sulfur.

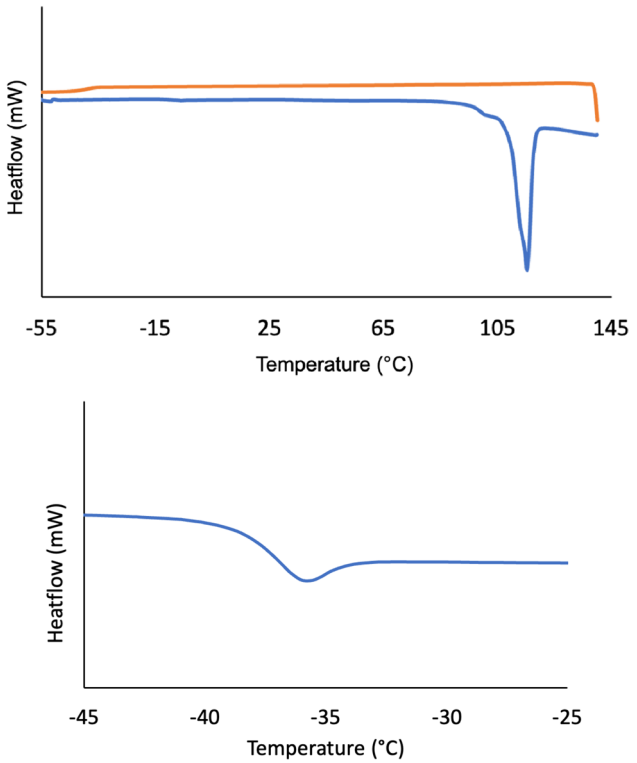

Fig. 6 DSC thermogram (top) for **LOS$_{90}$** (first heating cycle (blue line) and first cooling cycle (orange line)). The bottom image is an inset that more clearly reveals the glass transition temperature (T_g) observed in the third heating cycle. Endothermic transitions are downward in these thermograms (Color figure online)

Mechanical Properties and Environmental Impact Considerations

Elucidating the mechanical properties of **LOS$_{90}$** (Table 2) was undertaken to assess its viability as an alternative to less sustainable materials. Previous work [27–29] has shown that HSMs often have compressive strengths competitive with legacy mineral products used in structural applications. For example, ordinary Portland cement (OPC) generally has a flexural strength greater than 3 MPa and is required to have a compressive strength greater than 17 MPa to meet minimum specifications for use in residential building foundations according to American Concrete Institute code ACI 332.1R-06. Published data on the compressive strengths of sulfur-lignin derivative composites in particular are limited. The compressive strength of **LOS$_{90}$** (22.1 MPa, Fig. 7 and Table 2, stress–strain plots are provided in Fig. S67) exceeded the 17 MPa requirement. The compressive strength of **LOS$_{90}$** is also similar to those of composites comprising 10 wt. % whole lignin derivative and 90 wt. % sulfur (Table 2), for example **ELS$_{90}$@180** (20.1 MPa) and **ELS$_{90}$@230** (26.8 MPa), while being considerably higher than that of **ELS$_{80}$@180** (10.9 MPa) [13]. The preparation of **ELS$_x$@T** precursor oleic-esterified lignin is a much more energy and time-intensive process than that used to prepare the lignin oil required for **LOS$_{90}$** preparation, so **LOS$_{90}$** is a more viable construct for attaining similar compressive strength characteristics. It also valuable to compare the cost of bulk sulfur to the cost of ordinary Portland cement. When purchased at scale (as of February 26, 2024), bulk sulfur can be purchased for $80 per metric ton and lignin for $100 per metric ton (all costs are provided in USD). Taking the 64% conversion of whole lignin to lignin oil, making one ton of **LOS$_{90}$** requires 0.16 tons of whole lignin to give the 0.1 tons of lignin oil to combine with the 0.9 tons of sulfur, for a material cost of $88 per metric ton, somewhat lower than the average price of OPC ($130 per metric ton) [30]. These material cost estimates do not include the ethanol for use in lignin oil production (ethanol would be recovered for reuse on an industrial scale) or the water used for OPC curing. The comparable material costs are promising especially in light of ongoing rising costs of unsustainable resources.

The flexural strength and moduli of **LOS$_{90}$** was tested and evaluated, revealing high flexural strength (5.7 MPa) and moduli (186 MPa) at room temperatures compared to previously reported lignin sulfur composites (Table 2, stress–strain curves are provided in Fig. S68). The aforementioned **ELS$_x$@T** composites, for example, had flexural strengths of 2.7–3.9 MPa. Composites **LS$_x$** (x = wt. % sulfur), prepared by inverse vulcanization of allylated lignin,

Table 2 Mechanical properties of the lignin-sulfur composites **LOS_{90}** with comparison to other composites

Materials	Compressive strength (MPa)	Flexural strength/ modulus (MPa)	Compressive strength (% of OPC)	References
LOS_{90}[a]	22.1 ± 2.5	5.7/186	130	
LS_{80}[b]	ND	2.1/87	ND	[13]
LS_{85}[b]	ND	1.5/76	ND	[13]
LS_{90}[b]	ND	1.7/57	ND	[13]
LS_{95}[b]	ND	ND	ND	[13]
LS_{99}[b]	ND	ND	ND	[13]
GS_{80}[c]	ND	ND	ND	[15]
ELS_{90}@180[d]	20.1 ± 2.3	3.3/ND	118	[14]
ELS_{90}@230[d]	26.8 ± 0.5	3.9/ND	158	[14]
ELS_{80}@180[d]	10.9 ± 0.85	2.7/ND	64	[14]
CLS_{80}[e]	ND	3.6/ND	ND	[14]
$mAPS_{95}$[f]	17.0	5.6/ND	100	[41]
OPC[g]	17.0	3.7/580	100	[31]
S-DCPD (1:1)[h]	ND	6.0/3700	ND	[42]
S-DCPD-linseed oil (2:1:1)[i]	ND	4.7/1250	ND	[42]
S-DCPD-limonene (2:1:1)[j]	ND	1.9/1750	ND	[42]

[a]Lignin Oil (10 wt. %) and elemental sulfur (90 wt. %)

[b]**LS_x** composites consisting of 10 wt. % allyl-derivatized lignin and elemental sulfur where x = wt. % sulfur in monomer feed, varied from 80 to 99

[c]Composites consisting of guaiacol (20 wt. %) and elemental sulfur (80 wt. %)

[d]**ELS_x@T** composites consisting of esterified lignin and elemental sulfur where x = wt. % sulfur in the reaction mixture, varied from 80 to 90, and T is the reaction temperature in °C

[e]Composites consisting of chlorolignin (20 wt. %) and elemental sulfur (80 wt. %)

[f]Composites consisting of allyl lignin (2 wt. %), allyl cellulose (3 wt. %) and elemental sulfur (95 wt. %)

[g]Ordinary Portland Cement

[h]Composites consisting of elemental sulfur (50 wt. %) and dicyclopentadiene (DCPD) (50 wt. %)

[i]Composites consisting of elemental sulfur (50 wt. %), DCPD (25 wt. %), and linseed oil (25 wt. %)

[j]Composites consisting of elemental sulfur (50 wt. %), DCPD (25 wt. %), and limonene (25 wt. %)

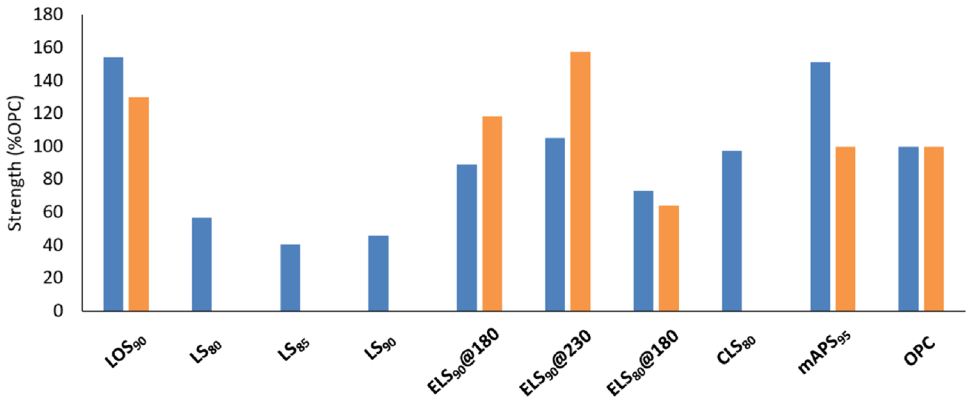

Fig. 7 Comparison of flexural strength (blue bars) and compressive strength (orange bars) of **LOS_{90}** with lignin-sulfur composites (**LS_x**), lignin/cellulose containing sulfur composites (**ELS_x@T**, **CLS_{80}**, **$mAPS_{95}$**), normalized to values of ordinary Portland Cement (17 MPa for compressive strength and 3.5 MPa for flexural strength). Bars not displayed indicate that the attendant value was not previously reported for the material listed (Color figure online)

showed flexural strengths (1.5–2.1 MPa) of less than 50% that of **LOS$_{90}$** and moduli of 57–87 MPa. A chlorolignin-sulfur composite (**CLS$_{80}$**) comprising 80 wt. % sulfur and 20% chlorolignin likewise exhibits somewhat lower flexural strength (3.6 MPa) than that of **LOS$_{90}$**. Whereas the flexural strength of **LOS$_{90}$** exceeds those of other sulfur-lignin HSMs comprising high (80–90 wt. %) sulfur, a similar flexural strength of 5.6 MPa has been reported for **mAPS$_{95}$** (prepared by inverse vulcanization of 2 wt. % allyl lignin, 3 wt. % allyl cellulose, and 95 wt. % sulfur). The flexural strength and modulus has also been reported for other high sulfur polymers with organic crosslinkers. Dicyclopentadiene (DCPD), a cheap industrial by-product, was reacted with elemental sulfur to form **S-DCPD** (50 wt. % sulfur and 50 wt. % dicyclopentadiene) [31]. The flexural strength of **LOS$_{90}$** (5.7 MPa) compares fairly to **S-DCPD** which exhibits a flexural strength of 6.0 MPa. However, when organic crosslinkers are incorporated with **S-DCPD**, the flexural strength decreases. When linseed oil is reacted with sulfur and DCPD to form **S-DCPD-linseed** (50 wt. % S, 25 wt. % dicyclopentadiene, 25 wt. % linseed oil), a slightly lower flexural strength of 4.7 MPa is observed. However, when limonene, a low-cost biomass material, was reacted with sulfur and DCPD to form **S-DCPD-limonene** (50 wt. % sulfur, 25 wt. % dicyclopentadiene, 25 wt. % limonene), a significantly lower flexural strength of 1.9 MPa was observed. However, the flexural moduli of **S-DCPD** (3700 MPa), **S-DCPD-linseed** (1250 MPa), and **S-DCPD-limonene** (1750 MPa) [31] greatly exceed that of **LOS$_{90}$** (186 MPa). It is also important to note that **LOS$_{90}$** exceeds the flexural strength of OPC (3.7 MPa), making it competitive with commercial building materials in this regard as well.

The viscoelastic properties of **LOS$_{90}$** were assessed using dynamic mechanical analysis (DMA). DMA data (Table 3 and Fig. S69 in the Supporting Information) were collected over the temperature range of –60 to + 80 °C in order to analyze the temperature dependence of storage modulus (E'), loss modulus (E''), and the damping factor (tan δ). The T_g values of –38, –38, and –40 °C observed from tan δ (local maximum), loss modulus (local maximum) and storage modulus (inflection point) agree well with the T_g of –36 °C observed from DSC data (Fig. 6 and Table 1). The transitions observed above 20 °C in both the storage and loss moduli curves are attributable to chain freedom of relative movement in less-ordered parts of the polymer film, [32] a feature observable for **LS$_{90}$** [12] and several other HSMs [33, 34] comprising polymeric sulfur chains as crosslinkers similar to those in **LOS$_{90}$**.

Table 3 Data from dynamic Mechanical Analysis of storage modulus (E'), loss modulus (E'') and damping factor (tan δ) from –60 to 80 °C

	Sulfur	LOS$_{90}$
E' at 20 °C (MPa)	295 [12]	504
tan δ T_g (°C)	NA	–38
E' T_g (°C)	NA	–40
E'' T_g (°C)	NA	–38

The *E* factor [35] is a useful metric for estimating of the relative greenness a chemical process, where *E* factor is equal to mass of waste produced divided by mass of useful product produced, such that a lower *E* factor is more desirable. Considering the process as beginning with whole lignin and elemental sulfur, an *E* factor of 0.057 was calculated for **LOS$_{90}$**, with the waste generated being lignin char left behind from the whole lignin not converted to the oil. The *E* factor was calculated according to the following equation:

$$E\text{factor} = \frac{\text{waste}}{\text{usefulproduct}} = \frac{\text{ligninchar}}{(\text{LOS}_{90})} = \frac{2.81\text{g}}{(49.25\text{g})} = 0.057$$

The ethanol used is recovered by distillation for reuse, so is not considered as a waste product in this calculation. Other sulfur-lignin derivative composites have *E* factors that are 1–2 orders of magnitude higher (Table 4) and produce notably more environmentally detrimental waste products than the insoluble lignin char that is the only waste material resulting from **LOS$_{90}$** synthesis. For comparison, the E factors for bulk chemicals range from < 1 to over 50 [36]. All of the *E* factors for sulfur-lignin derivative composites are notably lower than that of OPC, however. The *E* factor for **LOS$_{90}$** is also over an order of magnitude lower than that of OPC (1.4) [36]. Moreover, the primarily waste product of Portland cement production is CO_2, with about 1 kg of CO_2 released for every kilogram of cement produced, such that Portland cement production is responsible for ~ 8% of all anthropogenic CO_2 production [37]. These data emphasize the potential of waste-derived cements or geopolymer cements [38, 39] to replace legacy building materials in a future green economy.

Table 4 *E* factors for reported sulfur-lignin derivative composites

Material	*E* factor	Primary waste produced	Solvents used	References
LOS$_{90}$	0.057	Lignin char	Ethanol	This work
LS$_{90}$	0.5	Allyl bromide, allyl alcohol, NaBr, CO_2	Water, acetone, hexanes	[13]
ELS$_{90}$@T	2.13	Oleic acid, NaCl, CO_2, Dodecylbenzene sulfonic acid, *p*-toluene sulfonic acid	Water	[14]

Conclusion

Lignin oil made at low temperature (100 °C) in ethanol, a preferred green solvent, undergoes reaction with fossil fuel waste sulfur at 230 °C for two hours. The resulting composite, **LOS_{90}**, has compressive and flexural strengths exceeding those required for use in load-bearing components of the built environment. The method described herein for preparing **LOS_{90}** satisfies numerous facets of the Principles of Green Chemistry, such as achieving a 98.5% atom economy from lignin oil and sulfur to the product, thereby minimizing waste and facilitating the complete integration of reactants into the final product. Moreover, this method uses ethanol, a green solvent, utilizes renewable plant-derived lignin, and provided a valuable avenue for sulfur utilization. Given that OPC has high blue and grey water footprints and its manufacture accounts for 8% of anthropogenic CO_2, accomplishing this greener synthesis of a material having compressive strength appropriate for replacing OPC in some structural applications also holds promise for greener construction practices in the future. In addition to the fundamental chemical and mechanical tests reported herein, however, biological and environmental studies on toxicity and the potential of the materials for soil acidification should to be undertaken by those seeking to use the new composites in specific contexts to validate the safety of materials in those proposed applications.

Supplementary Information The online version contains supplementary material available at https://doi.org/10.1007/s10924-024-03287-5.

Acknowledgements This research is funded by the National Science Foundation grant number CHE-2203669 awarded to RCS.

Author Contributions KAT, NLKD, and CPM: data curation, formal analysis, investigation, validation. KAT and RCS: writing – original draft. RCS: conceptualization, funding acquisition, methodology, resources, supervision. NLKD: writing – review and editing.

Funding Open access funding provided by the Carolinas Consortium. The authors have not disclosed any funding.

Data Availability All data generated or analyzed during this study are included in this published article [and its supplementary information files].

Declarations

Conflicts of interest There are no conflicts to declare.

Ethical Approval This contribution does not contain any human and/or animal studies.

References

1. Wang C, Kelley SS, Venditti RA (2016) Chemsuschem 9:770–783
2. Zoia L, Salanti A, Frigerio P, Orlandi M (2014) BioResources 9:6540–6561
3. Crestini C, Lange H, Sette M, Argyropoulos DS (2017) Green Chem 19:4104–4121
4. Rinaldi R, Jastrzebski R, Clough MT, Ralph J, Kennema M, Bruijnincx PC, Weckhuysen BM (2016) Angew Chem Int Ed Engl 55:8164–8215
5. Sun Z, Fridrich B, de Santi A, Elangovan S, Barta K (2018) Chem Rev 118:614–678
6. Janicka P, Płotka-Wasylka J, Jatkowska N, Chabowska A, Fares MY, Andruch V, Kaykhaii M, Gębicki J (2022) Curr Opin Green Sustain Chem 37:100670
7. Tekin K, Hao N, Karagoz S, Ragauskas AJ (2018) Chemsuschem 11:3559–3575
8. Kouris PD, van Osch DJGP, Cremers GJW, Boot MD, Hensen EJM (2020) Sustainable Energy Fuels 4:6212–6226
9. Jessop PG (2011) Green Chem 13:1391–1398
10. Zhang X, Tang Y, Qu S, Da J, Hao Z (2015) ACS Catal 5:1053–1067
11. Lim J, Pyun J, Char K (2015) Angew Chem Int Ed 54:3249–3258
12. Karunarathna MS, Lauer MK, Thiounn T, Smith RC, Tennyson AG (2019) J Mater Chem A 7:15683–15690
13. Karunarathna MS, Maladeniya CP, Lauer MK, Tennyson AG, Smith RC (2023) RSC Adv 13:3234–3240
14. Karunarathna MS, Lauer MK, Smith RC (2020) J Mater Chem A 8:20318–20322
15. Yan P, Zhao W, Tonkin SJ, Chalker JM, Schiller TL, Hasell T (2022) Chem Mater 34:1167–1178
16. Karunarathna MS, Tennyson AG, Smith RC (2020) Facile new approach to high sulfur-content materials and preparation of sulfur–lignin copolymers. J Mater Chem A 8(2):548–553. https://doi.org/10.1039/C9TA10742H
17. Thiounn T, Karunarathna MS, Lauer MK, Tennyson AG, Smith RC (2023) RSC Sustainability 1:535–542
18. Kapuge Dona NL, Maladeniya CP, Smith RC (2024) Eur J Organ Chem n/a:e202301269
19. Dale JJ, Petcher S, Hasell T (2022) ACS Appl Polym Mater 4:3169–3173
20. Smith AD, Thiounn T, Lyles EW, Kibler EK, Smith RC, Tennyson AG (2019) J Poly Sci A 57:1704–1710
21. Dale JJ, Stanley J, Dop RA, Chronowska-Bojczuk G, Fielding AJ, Neill DR, Hasell T (2023). Eur Polymer J. https://doi.org/10.1016/j.eurpolymj.2023.112198,112198
22. Rao CNR, Venkataraghavan R, Kasturi TR (1964) Can J Chem 42:36–42
23. Derr KM, Lopez CV, Maladeniya CP, Tennyson AG, Smith RC (2023) J Polym Sci 61:3075
24. Derr KM, Smith RC (2023) J Polym Sci. https://doi.org/10.1002/pol.20230724, in press
25. Li L, Van de Vijver R, Van Geem KM (2023) Energy Fuels 37:7246–7259

26. Brebu M, Vasile C (2010) Cellul Chem Technol 44:353–363
27. Lopez CV, Karunarathna MS, Lauer MK, Maladeniya CP, Thiounn T, Ackley ED, Smith RC (2020) J Poly Sci 58:2259–2266
28. Lopez CV, Smith AD, Smith RC (2023) Macromol Chem Phys 9:2300233
29. Lopez CV, Smith RC (2023) J Appl Polym Sci. https://doi.org/10.1002/app.54828, e54828
30. S. R. Department, Cement Prices in The United States from 2010 to 2022 (in U.S. Dollars per Metric Ton), https://www.statista.com/statistics/219339/us-prices-of-cement/. Accessed 26 Feb 2024
31. Lopez CV, Smith AD, Smith RC (2022) RSC Adv 12:1535–1542
32. Liu Z, Maréchal P, Jérôme R (1997) Polymer 38:4925–4929
33. Thiounn T, Lauer MK, Bedford MS, Smith RC, Tennyson AG (2018) RSC Adv 8:39074–39082
34. Karunarathna MS, Lauer MK, Tennyson AG, Smith RC (2020) Polym Chem 11:1621–1628
35. Sheldon RA (2007) Green Chem 9:1273–1283
36. Phan TVT, Gallardo C, Mane J (2015) Green Chem 17:2846–2852
37. Turner LK, Collins FG (2013) Constr Build Mater 43:125–130
38. Furtos G, Molnar L, Silaghi-Dumitrescu L, Pascuta P, Korniejenko K (2022) J Nat Fibers 19:6676–6691
39. Furtos G, Silaghi-Dumitrescu L, Pascuta P, Sarosi C, Korniejenko K (2021) J Nat Fibers 18:285–296
40. Lauer MK, Estrada-Mendoza TA, McMillen CD, Chumanov G, Tennyson AG, Smith RC (2019) Adv Sustainable Syst 3:1900062
41. Lauer MK, Karunarathna MS, Tennyson AG, Smith RC (2020) Mater Adv 1:590–594
42. Smith JA, Green SJ, Petcher S, Parker DJ, Zhang B, Worthington MJH, Wu X, Kelly CA, Baker T, Gibson CT, Campbell JA, Lewis DA, Jenkins MJ, Willcock H, Chalker JM, Hasell T (2019) Chem Eur J 25:10433–10440